Proceedings of the IASTED International Conference.
International Conference on Modelling and Simulation.
May 5-8, 1999. Philadelphia. USA.

AN ENERGY RELAXATION TIME MODEL FOR DEVICE SIMULATION

B. GONZALEZ*, V. PALANKOVSKI**, H. KOSINA**,
A. HERNANDEZ*, and S. SELBERHERR**

*University Institute for Applied Microelectronics, Las Palmas de G.C.
Campus Universitario de Tafira, E-35017 Gran Canaria, SPAIN
Phone: +34/928/452875, Fax: +34/928/451243
E-mail: benito@cma.ulpgc.es

**Institute for Microelectronics, TU Vienna
Gusshausstrasse 27–29, A-1040 Vienna, AUSTRIA

ABSTRACT

We present an empirical model for the electron energy relaxation time. It is based on Monte-Carlo simulation results, and is applicable to all relevant diamond and zinc-blende structure semiconductors. The energy relaxation times are expressed as a function of the carrier and lattice temperatures, and in the case of semiconductor alloys, the material composition.

keywords: energy relaxation time, simulation, models, compounds, devices.

1 INTRODUCTION

As scaling down of the transistor's gate length is progressing, more appropriate models taking into account non-local effects are necessary [1, 2]. It is well known that for submicron structures, the classic drift-diffusion transport equations are insufficient to describe properly the physical behavior. Energy transport equations are necessary to model the increase of the carrier temperature at high electric fields [3]. Non-local effects, such as overshoot or real space transfer, must be reproduced.

A constant energy relaxation time (τ_w), or a quadratic dependence on the electron temperature [4, 5], are usually assumed. A precise simulation needs to include the dependence of τ_w on the lattice and carrier temperatures.

In this paper we present a new analytical model for the electron energy relaxation time based on Monte-Carlo results [6]. The dependence on the lattice and electron temperatures has been considered, and also the material composition for the semiconductor alloys. No doping concentration influence is taken into account. In section 2 the used methodology is explained. The new model is presented in section 3. It is applied to Si, Ge and III-V binary materials, and is also extended to semiconductor alloys.

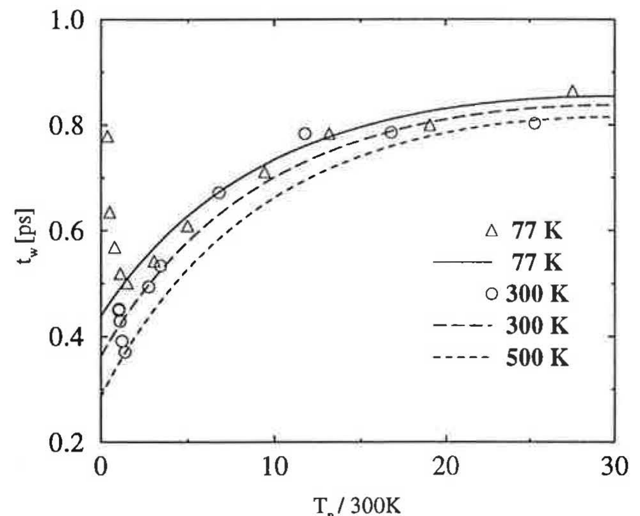

Figure 1: *MC data and our model applied to Si.*

2 METHODOLOGY

Depending on the semiconductor under investigation, different results are available from Monte-Carlo results. Two methods - direct and indirect - are used to obtain τ_w. A detailed explanation follows in the next subsections.

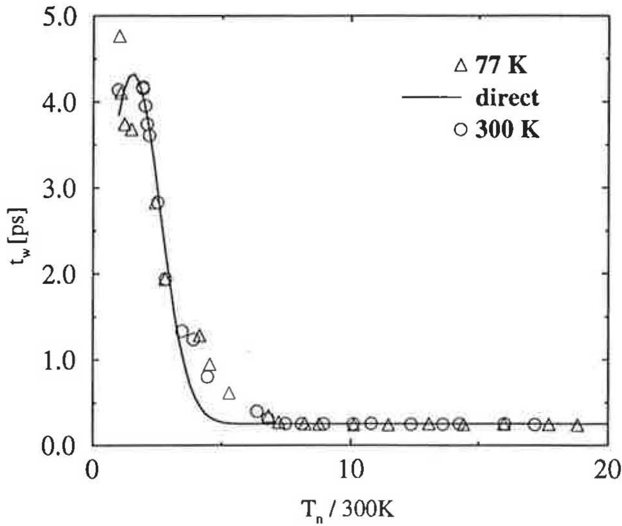

Figure 2: *MC data and our model applied to Ge.*

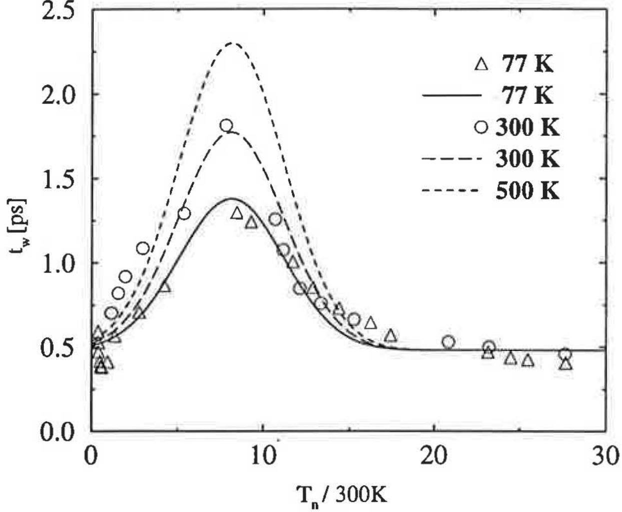

Figure 3: *MC data and our model applied to GaAs.*

2.1 THE DIRECT METHOD

For Si, Ge and GaAs, the dependence of the electron energy relaxation time and the average electron energy, w, on the electric field are available in [6]. The average energy is approximated by the thermal energy, with the kinetic term being neglected:

$$w = \frac{1}{2}m_n \cdot {v_n}^2 + \frac{3}{2}k_B \cdot T_n \approx \frac{3}{2}k_B \cdot T_n \qquad (1)$$

where m_n, v_n, and T_n are the electron mass, velocity and temperature, respectively, and k_B is the Boltzmann constant.

This approximation, together with the interpolation of the Monte-Carlo results for different electric fields, allow to obtain directly τ_w as a function of the electron temperature at different lattice temperatures. The lattice-temperature dependence is then added in a straight forward way to τ_w. This procedure is called direct method. The results for Si, Ge and GaAs are shown in Figs. 1, 2 and 3 respectively.

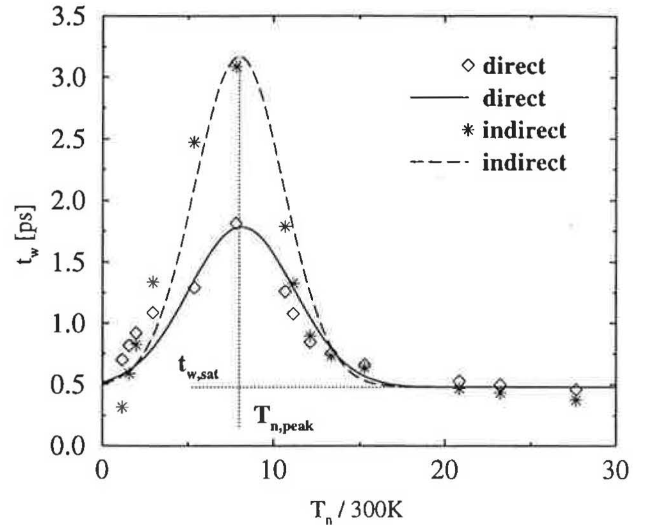

Figure 4: *Results from direct and indirect method.*

2.2 THE INDIRECT METHOD

In the case of binary and ternary III-V compounds, such as InAs, AlAs, $In_xGa_{1-x}As$, and $Al_xGa_{1-x}As$, the dependence of τ_w on the electric field is not available. In this case we calculate τ_w in an indirect way, using the dependence of the electron velocity on the electric field from [6]. The local energy balance equation [7] is obtained by neglecting the energy flux:

$$\tau_w = \frac{3 \cdot k_B}{2 \cdot q} \cdot \frac{T_n - T_L}{v_n \cdot E} \qquad (2)$$

where q is the electron charge, T_L the lattice temperature, and E is the electric field.

Using Eq. 1 and the dependences of the average electron energy and the electron velocity on the electric field, τ_w is extracted. By using Eq. 2, τ_w is overestimated. We assume the following criteria to compensate this overestimation. In Fig.4, τ_w for GaAs is shown as a function of the electron temperature at $300K$, as it results from both the direct and indirect methods. We can see that the saturation value of τ_w at high electron temperatures, $\tau_{w,sat}$, and the location of the peak, $T_{n,peak}$, are independent of the methodology used.

The energy relaxation time in $In_xGa_{1-x}As$ and $Al_xGa_{1-x}As$ τ_w behaves similarly to GaAs (see Figs. 5 and 6). We model τ_w for the III-V semiconductor alloys in that the height and the width of the Gaussian obtained for GaAs are maintained, while the lateral and vertical offsets, $T_{n,peak}$ and $\tau_{w,sat}$ respectively, are made composition-dependent.

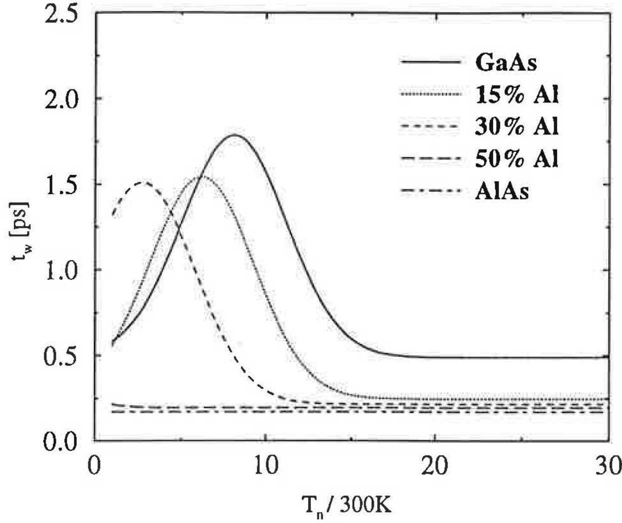

Figure 5: τ_w *for different Al contents in AlGaAs.*

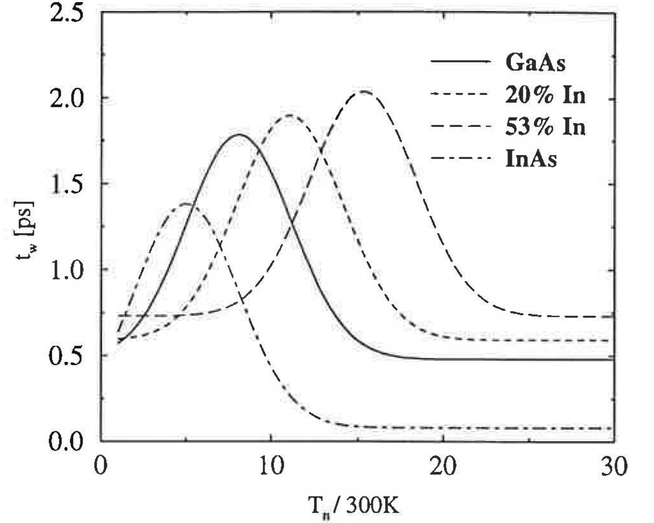

Figure 6: τ_w *for different In contents in InGaAs.*

3 THE RELAXATION TIME MODEL

We use the following Gaussian function to model the electron relaxation time as function of the carrier and lattice temperatures:

$$\tau_w = \tau_{w,0} + \tau_{w,1} \cdot \exp\left[C_1 \cdot \left(\frac{T_n}{300\ \mathrm{K}} + C_0\right)^2 + \right.$$
$$\left. + C_2 \cdot \left(\frac{T_n}{300\ \mathrm{K}} + C_0\right) + C_3 \cdot \left(\frac{T_L}{300\ \mathrm{K}}\right)\right] \quad (3)$$

The flexibility of this function allows its easy adaptability to all materials. For Si, Ge, and III-V binary materials, Table 1 shows all parameters in Eq. 3. In the case of III-V semiconductor alloys, the material composition (x) dependence of τ_w is included. It is modeled with $\tau_{w,0}$ and C_0 as a function of x, in the way explained in section 2.2. The parameters are summarized in Table 2.

3.1 ELEMENTARY AND BINARY SEMICONDUCTORS

The direct method is used for Si, Ge and GaAs, and the indirect one for AlAs and InAs. The resulting parameters are shown in Table 1.

For Si we can see in Fig.1 the values for τ_w obtained from the model (lines) and Monte-Carlo results (circles and triangles) at different lattice temperatures. The energy relaxation time slightly decreases with the increase of the lattice temperature. It is also observed that for high electron temperatures, τ_w tends to saturate.

At very low electron temperature τ_w starts increasing. This effect is not reproduced by the model. When the electron temperature is close to the lattice temperature, the term $\frac{T_n - T_L}{\tau_w}$ appearing in the energy balance tends to zero [4]. The influence of the electron temperature on τ_w is much more important at high electric fields, and therefore this effect is neglected.
In GaAs and Ge similar behavior was observed at very low electron temperatures, and the same assumptions as for Si were made.

In the case of Ge, Fig.2 shows that τ_w is nearly independent of the lattice temperature, except for very low electron temperature. Therefore, any lattice temperature dependence is neglected ($C_3 = 0$ in Eq. 3). The sharp initial fall is attributed to the increasing of optical and inter valley scattering as the electrons are heated by the field [8].

The results for GaAs are shown in Fig.3. At high electron temperatures τ_w tends to some saturated value and becomes independent of the lattice temperature. For low-intermediate electron temperatures, the behavior can be attributed to the transition of electrons from the Γ to the L valleys. The electron temperature, for which τ_w reaches the peak value, is in-

Material	$\tau_{w,0}$	$\tau_{w,1}$	C_0	C_1	C_2	C_3
Si	1.0	-0.538	0	0.0015	-0.09	0.17
Ge	0.26	1.49	0	-0.434	1.322	0
GaAs	0.48	0.025	0	-0.053	0.853	0.5
AlAs	0.17	0.025	61	-0.053	0.853	0.5
InAs	0.08	0.025	3	-0.053	0.853	0.5

Table 1: Parameter values for non-alloy materials. $\tau_{w,0}$ and $\tau_{w,1}$ are given in ps, the rest are unitless.

dependent of the lattice temperature. The associated average energy, 0.31 eV (Eq. 1), is close to the energy difference between the two valleys, 0.27 eV.
The lattice temperature dependence of τ_w is reverse to the one observed in Si.

3.2 SEMICONDUCTOR ALLOYS

For III-V semiconductor alloys, $A_xB_{1-x}C$, a quadratic interpolation is used to calculate $\tau_{w,0}$ and C_0. The interpolation is taken between the values of the binary compounds, AC and BC, from Table 1. Therefore we have:

$$\tau_{w,0}^{ABC} = \tau_{w,0}^{AC} \cdot x + \tau_{w,0}^{BC} \cdot (1-x) + \tau_{w,o}^{*} \cdot (1-x) \cdot x$$

$$C_0^{ABC} = C_0^{AC} \cdot x + C_0^{BC} \cdot (1-x) + C_o^{*} \cdot (1-x) \cdot x (4)$$

$\tau_{w,o}^{*}$ and C_o^{*} are referred to as nonlinear or bowing parameters. The parameters used in this model are summarized in Table 2. $\tau_{w,o}^{*}$ are is given in picoseconds, and C_o^{*} is unit less.

Material	$\tau_{w,o}^{*}$	$\tau_{w,1}$	C_o^{*}	C_1	C_2	C_3
AlGaAs	-0.35	0.025	-61	-0.053	0.853	0.5
InGaAs	1.8	0.025	-34	-0.053	0.853	0.5

Table 2: Parameter values for alloy materials. $\tau_{w,0}$ and $\tau_{w,1}$ are given in ps, the rest are unitless.

The indirect method is used for all semiconductor alloys, as explained in section 2.2. The lattice temperature dependence of τ_w of GaAs is preserved for both semiconductor alloys considered, $Al_xGa_{1-x}As$ and $In_xGa_{1-x}As$. This approximation is better accurate for low material composition, that is the most frequently used ($x < 0.3$).

Fig.5 shows the results of the model for $Al_xGa_{1-x}As$ at 300 K for different material compositions. Note the shift of the electron temperature, giving the peak of τ_w, to lower values with the increase of the aluminum material composition, x. For high values ($x = 0.5, 1$) no peak value of τ_w is observed. This behavior can be attributed to the conduction band dependence on x of the Γ, L and X valleys [6]. When the aluminum composition changes from 0 to 0.3, the band gap energy between the Γ and L valleys varies between 0.27 and 0.1 eV. It was observed that the corresponding change of the electron energy associated to the peak of τ_w (Eq. 1), varies between 0.31 to 0.1 eV. Furthermore, for an aluminum material composition higher than $x = 0.4$, the X valley is the lowest conduction band, changing the band gap from direct to indirect. No peak of τ_w is observed.

For $In_xGa_{1-x}As$ similar results are obtained in Fig.6. There is a shift of the maximum τ_w to higher values with the increasing of the indium composition up to $x = 0.53$. This can be explained properly with the electron population transition between Γ and L valleys [6]. But for InAs it is observed a quick shift to lower values, not explained with the energy conduction bands dependence on x. Monte Carlo results show that, when the indium composition is very high, the average electron energy starts decreasing and the saturation drift velocity increases very much, but no clear results are provided by [6] in this case.

4 CONCLUSIONS

A new electron energy relaxation time model for device simulation is presented. It is applied to the most widely used semiconductors, and takes into account the electron and lattice temperatures, and the material composition in the case of alloys. The good agreement with the Monte-Carlo results and its easy computational implementation, make it attractive for usage in device simulation.

References

[1] T. Grasser, V. Palankovski, G. Schrom, and S. Selberherr. Hydrodynamic Mixed-Mode Simulation. In K. De Meyer and S. Biesemans, editors, *Simulation of Semiconductor Processes and Devices*, pages 247–250. Springer, Wien, New York, 1998.

[2] A.S. Spinelli, A. Benvenuti, and A. Pacelli. Self-Consistent 2-D Model for Quantum Effects in n-MOS Transistors. *IEEE Trans.Electron Devices*, 45(6):1342–1349, 1998.

[3] T. Shawki, G. Salmer, and O. El-Sayed. MODFET 2-D Hydrodynamic Energy Modeling: Optimization of Subquarter-Micron-Gate Structures. *IEEE Trans.Electron Devices*, 37(1):21–30, 1990.

[4] H. Brech. *Optimization of GaAs Based High Electron Mobility Transistors by Numerical Simulation*. Dissertation, Technische Universität Wien, 1998.

[5] V.M. Agostinelli, T.J. Bordelon, X.L. Wang, C.F. Yeap, C.M. Maziar, and A.F. Tasch. An Energy-Dependent Two-Dimensional Substrate Current Model for the Simulation of Submicrometer MOSFETs. *IEEE Electron Device Lett.*, 13(11):554–556, 1992.

[6] M.V. Fischetti and S.E. Laux. Monte Carlo Simulation of Transport in Technologically Significant Semiconductors of the Diamond and Zinc-Blende Structures–Part II: Submicrometer MOSFET's. *IEEE Trans.Electron Devices*, 38(3):650–660, 1991.

[7] S.M. Sze. *Physics of Semiconductor Devices*. Wiley, New York, second edition, 1981.

[8] C. Jacoboni, F. Nava, C. Canali, and G. Ottaviani. Electron Drift Velocity and Diffusivity in Germanium. *Physical Review B*, 24(2):1014–1026, 1981.